

Effects of Neglecting Polarization on the MODIS Aerosol Retrieval Over Land

Robert C. Levy, Lorraine A. Remer, and Yoram J. Kaufman

Abstract—Reflectance measurements in the visible and infrared wavelengths, from the Moderate Resolution Imaging Spectroradiometer (MODIS), are used to derive aerosol optical thicknesses (AOTs) and aerosol properties over ocean and land surfaces, separately. Both algorithms employ radiative transfer (RT) code to create lookup tables, simulating the top-of-atmosphere (TOA) reflectance measured by the satellite. Whereas the algorithm over ocean uses a vector RT code that includes the effects of atmospheric polarization, the algorithm over land assumes scalar RT, thus neglecting polarization effects. In the red ($0.66\ \mu\text{m}$) and infrared ($2.12\ \mu\text{m}$) MODIS channels, scattering by molecules (Rayleigh scattering) is minimal. In these bands, the use of a scalar RT code is of sufficient accuracy to model TOA reflectance. However, in the blue ($0.47\ \mu\text{m}$), the presence of larger Rayleigh scattering (optical thickness approaching 0.2) results in nonnegligible polarization. The absolute difference between vector- and scalar-calculated TOA reflectance, even in the presence of depolarizing aerosols, is large enough to lead to substantial errors in retrieved AOT. Using RT code that allows for both vector and scalar calculations, we examine the reflectance differences at the TOA, assuming discrete loadings of continental-type aerosol. We find that the differences in blue channel TOA reflectance (vector–scalar) may be greater than 0.01 such that errors in derived AOT may be greater than 0.1. Errors may be positive or negative, depending on the specific geometry, and tend to cancel out when averages over a large enough sample of satellite geometry. Thus, the neglect of polarization introduces little error into global and long-term averages, yet can produce very large errors on smaller scales and individual retrievals. As a result of this study, a future version of aerosol retrieval from MODIS over land will include polarization within the atmosphere.

Index Terms—Aerosol, land, Moderate Imaging Spectroradiometer (MODIS), polarization, radiative transfer.

I. INTRODUCTION

ATMOSPHERIC aerosols are intimately linked to earth's climate system [1], hydrological cycle [2], and to the well being of earth's inhabitants [3]. However, aerosols are difficult to study on a global scale because they are inhomogeneous on all temporal, horizontal, and vertical scales. Satellite measurements are increasingly important to the study of aerosols in earth's

system [4], [5], because they can view large parts of the globe within a short time span. Passive sensors, such as the Moderate Imaging Spectroradiometer (MODIS) [6], flying aboard Terra [7] and Aqua [8], measure reflected radiation at the top of the atmosphere (TOA) and do not disturb the ambient aerosol composition. As compared to previous satellite sensors used for (but not designed for) aerosol retrieval (such as the Advanced Very High Resolution Radiometer (AVHRR; e.g., [9]), MODIS has a much wider spectral range ($0.412\text{--}15\ \mu\text{m}$), finer spatial resolution ($250\text{--}1000\ \text{m}$), and is calibrated to a much higher accuracy [10]. Thus, MODIS is a premier instrument for estimating the spectral aerosol optical thickness (AOT), leading to estimates of aerosol size parameters.

MODIS retrieves clear sky (noncloudy) aerosol optical thickness (AOT) over ocean and land, using two separate algorithms [11]–[14]. The ocean algorithm retrieves AOT in seven wavelength bands, centered near 0.47 , 0.55 , 0.66 , 0.87 , 1.24 , 1.64 , and $2.12\ \mu\text{m}$, by inverting reflectance in six of the seven bands ($0.47\ \mu\text{m}$ is contaminated by variable ocean surface reflectance and is not used in the retrieval). The land algorithm derives AOT in two bands (0.47 and $0.66\ \mu\text{m}$), by using reflectance in three bands (0.47 , 0.66 , and $2.12\ \mu\text{m}$), and then interpolates to find AOT at $0.55\ \mu\text{m}$. Therefore, both algorithms report the AOT at $0.55\ \mu\text{m}$ and an estimate of the spectral dependence of the AOT. Both algorithms make use of lookup tables (LUTs), wherein TOA spectral reflectance (in percent) is simulated by radiative transfer (RT) calculations. Included within the RT are assumptions about the surface reflectance, molecular scattering, and aerosol scattering/absorption (functions of assumed aerosol chemical and size parameters). For each cloud-screened MODIS pixel of suitable quality [14], the retrieval algorithm attempts to mimic the observed spectral reflectance with values from the LUT. Minimum total differences between the two spectral quantities lead to solutions of spectral AOT. Over ocean, the minimization is applied to the six wavelengths simultaneously, whereas over land, the minimization is applied to the 0.47- and $0.66\text{-}\mu\text{m}$ channels independently,

Ocean and land AOTs each have theoretical expected error bars [11], [12], which have been subsequently “validated” [14]–[17] by comparing to ground based sunphotometers, such as those of the AEROSOL ROBOTIC NETWORK (AERONET) [18]. Over nondusty ocean sites, global MODIS/AERONET AOT regression lines have slopes near one, offsets near zero, and correlation coefficients of 0.9 and above. Over land sites, the global MODIS/AERONET regression has an offset about 0.1, slope about 0.8, and correlation coefficients of about 0.6.

Why is the MODIS/AERONET comparison so much poorer over land surfaces? The fundamental strategy for each algorithm

Manuscript received May 20, 2004; revised August 30, 2004. This work was supported by the National Aeronautics and Space Administration's Earth Sciences as part of the MODIS Project.

R. C. Levy is with Science Systems and Applications, Inc., Lanham, MD 20771 USA, the Laboratory for Atmospheres, National Aeronautics and Space Administration, Goddard Space Flight Center, Greenbelt, MD 20771 USA and also with the Department of Meteorology, University of Maryland, College Park, MD 20742 USA (e-mail: levy@climate.gsfc.nasa.gov).

L. A. Remer and Y. J. Kaufman are with the Laboratory for Atmospheres, National Aeronautics and Space Administration, Goddard Space Flight Center, Greenbelt, MD 20771 USA (e-mail: remer@climate.gsfc.nasa.gov; kaufman@climate.gsfc.nasa.gov).

Digital Object Identifier 10.1109/TGRS.2004.837336

is different. The ocean is nearly black at red and longer wavelengths, so that the atmosphere can be assumed to dominate the TOA signal. The use of MODIS observations at multiple wavelengths allows the algorithm to match the spectral signatures of a particular aerosol size distribution [12]. Over the land, however, the surface is variable in space and time and can dominate the total signal. Not only must the surface properties be constrained, the retrieval is regulated to only the wavelengths where the surface appears dark. Thus, there are fewer available channels and greater uncertainty in estimating surface reflectance, meaning that the overland retrieval has insufficient information to match the spectral signature of a unique aerosol size distribution. Therefore, the aerosol model, as well as the surface reflectance properties, must be constrained when simulating the MODIS observation. Errors in the aerosol retrieval result from insufficient knowledge about the surface optical properties [19] and/or expected aerosol properties (i.e., single-scattering albedo [20]). These two sources of error are examined in [21] and will be studied further in future studies.

Another difference between the two algorithms is in their treatment of radiative transfer (RT) within the atmosphere. The overocean algorithm employs a vector radiative transfer code that includes polarization within the atmosphere, whereas the overland algorithm assumes that scalar RT is sufficient for simulating the MODIS observations. Under conditions of moderate Rayleigh (molecular) optical thickness (ROT) greater than 0.1, however, polarization within the atmosphere will modify the TOA radiance by 2% or more [22]. The MODIS aerosol algorithms use observations in the blue MODIS band (0.47 μm) where the sea-level ROT is nearly 0.2, e.g., [22], introducing errors of up to 4% [21]. In addition to the Rayleigh optical thickness, aerosol optical thicknesses of 0.2 or more are not uncommon. Aerosols tend to depolarize radiation; however, scalar/vector reflectance differences may still be important, inducing errors in aerosol retrieval.

In this paper, we address possible errors in TOA reflectance introduced by simulating MODIS overland observations by RT that neglects polarization in the atmosphere. Polarization of the land surface bidirectional reflectance function (BRDF) is beyond the scope of this paper. We introduce polarization in Section II and discuss how polarization is used and neglected within the MODIS aerosol retrieval in Section III. Section IV describes the RT modeling performed here, results of which are discussed as well. Implications to MODIS aerosol retrieval on both global and local scales are given in the conclusion section (Section V).

II. POLARIZATION IN THE ATMOSPHERE

To fully describe electromagnetic radiation at the TOA, one must use the Stokes vector \mathbf{I} composed of four Stokes parameters

$$\mathbf{I} = \{I, Q, U, V\}$$

where the scalar I represents the intensity (radiance) or reflectance (normalized radiance), and Q , U , and V describe the polarization state of the radiation. Incoming sunlight at the TOA is unpolarized, such that $\mathbf{I} = \{I, 0, 0, 0\}$. However, due to interaction with the surface and the atmosphere, reflected

light at the TOA generally becomes polarized (Q , U , and/or V are nonzero). The degree of polarization P is defined as

$$P = \frac{(Q^2 + U^2 + V^2)^{1/2}}{I}.$$

This means that radiation with polarization P can be decomposed into unpolarized and polarized components such that, for example, [23], [24]

$$\mathbf{I} = \mathbf{I}_{\text{Unpol}} + \mathbf{I}_{\text{Pol}} = [I(1 - P), 0, 0, 0] + [IP, Q, U, V]$$

and that intensity itself is

$$I = I_{\text{Unpol}} + I_{\text{Pol}} = I(1 - P) + IP.$$

If P is assumed equal to zero, this is known as the scalar approximation of RT transfer and results in estimating I by I_{Unpol} . In many applications of remote sensing, the scalar approximation is considered to be sufficient.

If P is large, however, substantial errors will be introduced by equating I with I_{Unpol} . It was first shown in [25] that radiance errors introduced by the scalar approximation can exceed 10% for Rayleigh scattering. Mishchenko *et al.* [22] provided expanded discussion and formal analysis of Rayleigh scattering errors in a plane-parallel atmosphere above a Lambertian surface. This study showed that the relative error of the TOA intensity decreased with increasing depolarization (arising from multiple scattering for example) and/or increasing surface albedo. For Rayleigh single-scattering albedo near unity (conservative scattering), maximum relative errors were observed at optical thickness near 1 and at scattering angles near 0° and 90° . These findings were attributed to the unique qualities of Rayleigh scattering.

The above studies quantified the relative errors when neglecting polarization when calculating TOA intensity in a pure Rayleigh atmosphere. However, they did not include the effect of aerosols, ubiquitous in the atmosphere. Additionally, they did not address how errors of the estimated intensity would lead to errors in remote sensing applications, such as retrieval of AOT.

III. MODIS ALGORITHM AND ITS NEGLECT OF POLARIZATION

If an instrument is sensitive to polarization, the measured intensity I_m is not necessarily equal to I . In the case of MODIS, it was determined prelaunch that sensitivity to polarization in the aerosol retrieval bands is small, resulting in differences between I_m and I less than 1%. Therefore, no correction should be needed to compare RT simulations with observations. However, scalar RT calculations may introduce artificial differences between I_m and simulated I that would introduce errors into retrieved aerosol properties.

The current LUT tables, derived for aerosol retrieval over land, were calculated using a scalar RT code, specifically the scalar version of the RT code formulated by Dave [26]. The use of the Dave code has long been a standard in the remote sensing community, desirable because it was well understood. It was also easily updated for use in creating the MODIS lookup tables. Polarization was not considered to be a major issue, because previous aerosol missions focused in the red and near-infrared

(NIR) wavelengths (e.g., 0.64 and 0.84 μm for AVHRR). In these wavelengths, where the Rayleigh optical thickness (ROT) is small (about 0.05 and 0.01, respectively), the inclusion of polarization would have made little difference to the simulated TOA reflectance (intensity). Indeed, differences in reflectance between Dave's vector and scalar codes [26] are less than 3% for wavelengths $\lambda \geq 0.64 \mu\text{m}$ [27].

In addition to the red and NIR wavelengths, however, MODIS makes use of reflectance in the blue (0.47 μm). Fraser *et al.* [27] pointed out that under conditions of large optical depths and large incident radiance, the increasing dominance of multiple scattering leads to larger errors in scalar assumed radiances. At this wavelength, the Rayleigh optical thickness is nearly 0.2. The addition of at least moderate AOT (say 0.2) would induce multiple scattering of the Rayleigh-induced polarization. The polarization factor would be reduced, so that the relative effect on the TOA radiance would be reduced from the 5% to 10% [21] for pure Rayleigh scattering. However, the increased AOT increases the TOA radiance, resulting in larger *absolute* errors in scalar assumed radiance. It is the absolute error in simulated reflectance (radiance), not the relative error, that introduces error into the derivation of AOT.

Mishchenko *et al.* [22] and Lacis *et al.* [28] suggested that a maximum relative error (in percent) of TOA intensity and sky radiance would occur when a pure molecular (Rayleigh) optical thickness is about 1, dependent on scattering geometry. Total optical thickness (aerosol plus Rayleigh) of 1 is not unusual in the blue, suggesting that whereas the TOA errors may not be as large as if for a pure Rayleigh atmosphere, polarization should still be included when creating the MODIS overland LUTs.

IV. ATMOSPHERIC POLARIZATION APPLIED TO AEROSOL RETRIEVAL

Our study analyzed how differences between vector- and scalar-derived TOA reflectance would lead to errors in retrieved AOT. For eight selected geometries and a variety of AOTs (representative of MODIS observations and the current LUT), we calculated TOA reflectance in both the blue (0.47 μm) and the red (0.66 μm) MODIS channels, using scalar and vector RT codes separately. The difference between the results was considered the scalar-derived reflectance error. For these same selected geometries and AOTs, we updated the (scalar-derived) LUT to reflect the additional reflectance arising from polarization. Using the revised (vector-derived) LUT, and setting the MODIS "observations" to values from the scalar LUT, we determined how the neglect of polarization would introduce errors in derived AOT.

A. Mie and RT Codes

For this exercise, we employed the polarized atmospheric radiative transfer model (RT3) of Evans and Stephens [29]. This plane-parallel adding/doubling code allows for polarization to be turned on or off by changing only one line within an input file. Thus, it was easy to determine differences in reflectance due only to polarization. The other inputs, including the wavelength, aerosol parameters, surface reflectance, and atmospheric profiles, were kept constant in both representations.

TABLE I
OPTICAL PROPERTIES OF THE CONTINENTAL AEROSOL MODEL. LISTED FOR EACH MODE ARE THE MEAN RADIUS r_v AND STANDARD DEVIATION σ OF THE VOLUME DISTRIBUTION. THE COMPLEX REFRACTIVE INDEX IS DEFINED AT 0.47 μm

Mode	r_v (μm)	σ	Refractive Index
Water Soluble	0.176	1.09	1.53-0.005i
Dust Like	17.6	1.09	1.53-0.008i
Soot	0.050	0.693	1.75-0.45i

We used the Mie vector (MIEV) code [30] to compute the aerosol optical properties offline. The same combination of RT3 and MIEV was also used in the dust studies of Colarco *et al.* [31].

B. Aerosol, Atmospheric, and Surface Properties

Aerosol optical properties were computed offline by MIEV. We used 3000 size bins, logarithmically spaced from $r_{\min} = 0.0084 \mu\text{m}$ to $r_{\max} = 56.042 \mu\text{m}$, having intervals of $d \cdot \ln(r) = 0.002937$. We modeled the "continental model" listed in [11] and described in [32]. This model is composed of three lognormal modes, properties for each are listed in Table I.

Mie outputs, necessary for RT3 calculation, included the extinction and scattering coefficients and coefficients of the scattering phase matrix (calculated for 750 moments).

For the atmospheric profile (temperature, pressure, humidity), we employed the U.S. midlatitude summer profile [33] at 36 levels between the surface and TOA. Aerosols were placed within this model atmosphere as an exponential distribution, having a scale height of 2 km. We assumed the land surface to be Lambertian and very dark vegetation (as may be found around Washington, DC), with spectral reflectance of 0.04 and 0.08 for blue (0.47 μm) and red (0.66 μm), respectively (e.g., [21]). The ROTs (at sea level) are about 0.194 and 0.051 for the two wavelengths, respectively. Within each layer of the MLS atmosphere, we combined weighted aerosol and molecular extinction to yield optical thicknesses and phase matrices. These weighted atmospheric columns were calculated for seven discrete values of AOT between 0.0 and 5.0.

C. TOA Spectral Reflectance

The TOA spectral reflectance was calculated by both the scalar and the vector implementations of the RT3 code, for the set of sun/surface/satellite geometrical conditions that were originally used for the operational lookup table [14]. We included nine solar zenith angles (between 0° and 60°), 11 sensor zenith angles (between 0° and 60°), and 31 relative sun/satellite azimuth angles (between 0° and 180° , for a total of 3069 geometrical combinations. The relative azimuth angle ϕ is defined in regard to the path of radiation; $\phi = 180^\circ$ indicates that the sun and satellite are viewed at the same azimuth from the surface, whereas $\phi = 0^\circ$ implies that they are opposite in the sky.

Plotted in Fig. 1 are the TOA blue-0.47 μm [Fig. 1(a)] and red-0.66 μm [Fig. 1(b)] differences (vector-scalar) in TOA reflectance, for eight geometries representative of MODIS geometry in the tropics and midlatitudes (Table II). At large optical

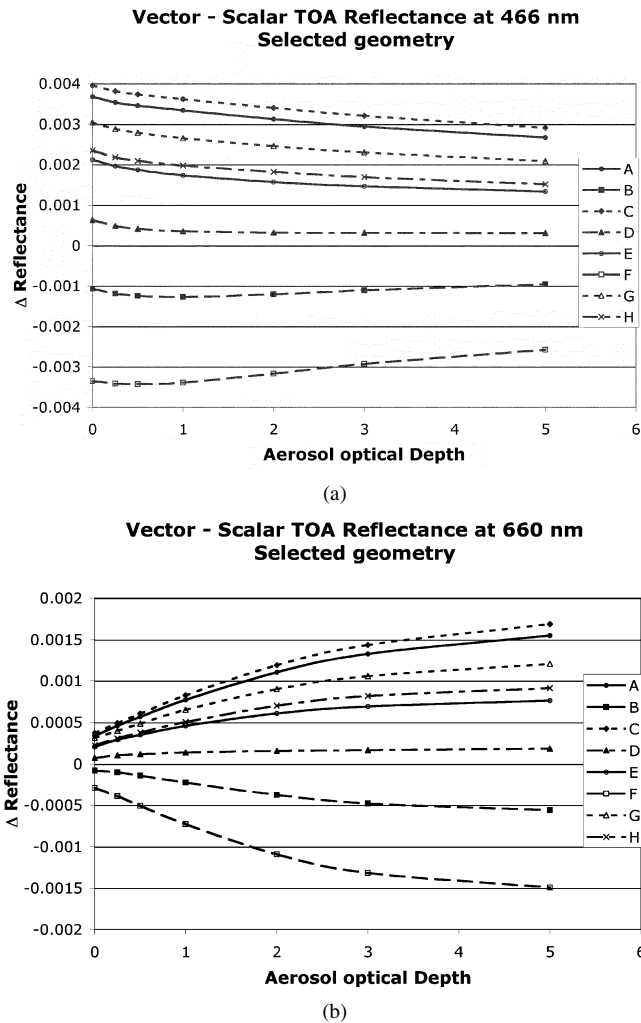


Fig. 1. Difference between vector- and scalar-derived reflectance at the TOA, for eight example sun/surface/satellite geometries, as a function of AOT. (a) At 0.466 μm , where the ROT = 0.194. (b) At 0.660 μm , where the ROT = 0.051. Details of the eight geometries are given in Table II.

TABLE II
SOLAR/SURFACE/SATELLITE GEOMETRY FOR EIGHT EXAMPLES.
ALL UNITS ARE DEGREES

Reference	Solar Zenith	View Zenith	Relative Azimuth	Scattering Angle
A	12.00	6.97	60.00	163.40
B	12.00	52.84	60.00	120.53
C	12.00	6.97	120.00	169.59
D	12.00	52.84	120.00	132.35
E	36.00	6.97	60.00	140.12
F	36.00	52.84	60.00	104.74
G	36.00	6.97	120.00	147.00
H	36.00	52.84	120.00	136.29

depths, the magnitude of the vector-scalar reflectance in the blue (~ 0.003) is about double of the red (~ 0.0015). However, in more normal aerosol loadings ($\tau = 0.25$), the differences in the blue (~ 0.004) are more like eight times those in the red (~ 0.0008).

Fig. 1 demonstrates that the sign of the vector/scalar reflectance difference can be either positive or negative. This is mainly a “function” of the scattering angle Θ , a result of the

relative positions of the sun, surface, and satellite. Fig. 2 displays contour plots of the vector/scalar difference as a function of solar and view zenith geometry, for two separate relative azimuth angles ($\phi = 30^\circ$ and 150°). Scattering angles are also plotted as contours. Generally, vector-scalar reflectance is positive when $\Theta > 135^\circ$ and negative when $\Theta < 135^\circ$. Magnitudes of the differences increase toward 180° and 90° , similar as would be expected from simulating a purely Rayleigh atmosphere, e.g., [22]. However, the contours are not necessarily parallel. Because upward and downward radiation paths are asymmetric, all angles must be considered, not just the scattering angle.

Fig. 3 plots the blue (0.47 μm) wavelength vector-scalar reflectance differences for all of the 3069 simulated geometries, as a function of scattering angle. Here, the AOT was set at 0.25. Due to the orbit of a polar-orbiting satellite such as MODIS, passing the equator close to noon, scattering angles less than 90° are rare. Again, it is seen that the scattering angle is the primary indicator of the sign of the polarization effect; however, the specific sun/surface/satellite geometry determines its magnitude.

D. Retrieval of AOT

For the above examples of solar and satellite geometry, absolute vector-scalar differences in the blue (0.47 μm) reflectances are often greater than 0.01 and may be as high as 0.03 for very large solar zenith angles. How much uncertainty would the erroneous TOA reflectance (calculated from the scalar approximation) introduce into the retrieval of AOT from MODIS?

For the eight selected geometrical conditions described in Table II, we have integrated the vector-scalar reflectance differences (plotted in Fig. 1) into the MODIS algorithm. Fig. 4 plots the change in retrieved AOT as a function of the inputted AOT, in the blue [Fig. 4(a)] and red [Fig. 4(b)] wavelengths. Positive differences in reflectance (plotted in Fig. 1) lead to negative errors in the retrieved AOT. Conceptually, this can be explained as follows. If at a particular AOT within the revised LUT, the new (polarized) reflectance value is larger than the old (scalar) value, then the retrieved AOT corresponding to the old value (used as input) must be lower.

In most cases, the magnitude of the AOT error is about ten times the magnitude of the reflectance error [34]. However, at some geometries and optical depths, the ratio can be much larger. Some examples include geometries “F” and “B” in the blue, where the AOT error is 30 times the reflectance difference at $\tau = 3.0$, and “G” and “A” (also in the blue), where the error is more than 20 times the difference at $\tau = 0.25$. It is impossible to tell if these are real “kinks” in Fig. 4(a) or if they are a result of numerical instability in the MODIS algorithm’s interpolation.

E. Influence of Errors Upon Retrieval of Aerosol Climatology

Whereas it is obvious that the neglect of polarization will induce large errors (either positive or negative) upon an individual aerosol retrieval, it is not so clear what effects neglecting polarization may have upon retrievals of aerosol climatology.

Fig. 5 displays the extreme, median, and quartile values of vector-scalar differences of TOA reflectance, for the entire set of

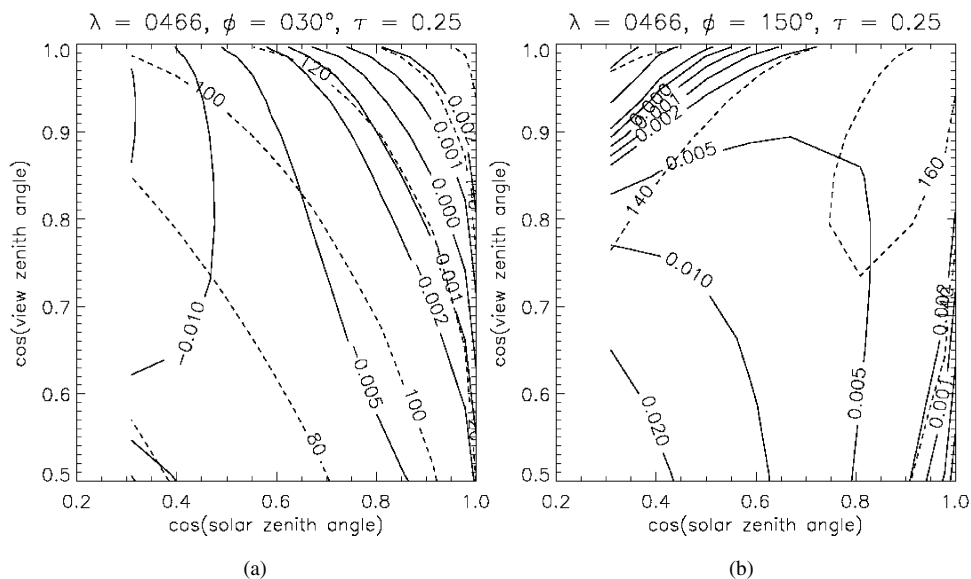


Fig. 2. Contour plots of the reflectance difference (vector-scalar) between RT3 calculations of TOA blue (0.466 μm) reflectance, as a function of view and solar zenith angles for two different relative azimuths. Contours of scattering angle are also plotted. AOT = 0.25 and ROT = 0.194. (a) $\phi = 30^\circ$. (b) $\phi = 150^\circ$. Note the signs of the contours.

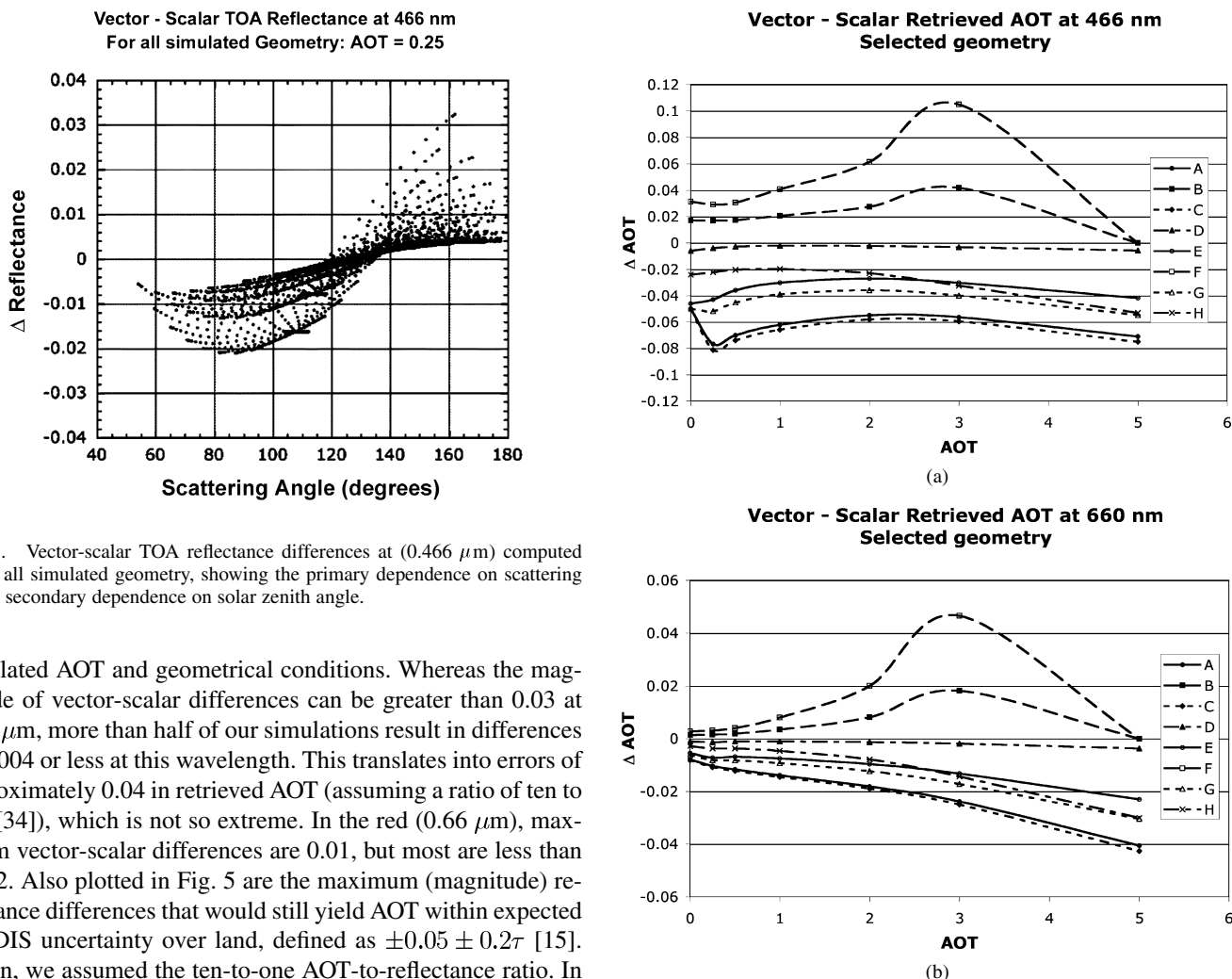


Fig. 3. Vector-scalar TOA reflectance differences at (0.466 μm) computed under all simulated geometry, showing the primary dependence on scattering angle, secondary dependence on solar zenith angle.

simulated AOT and geometrical conditions. Whereas the magnitude of vector-scalar differences can be greater than 0.03 at 0.47 μm, more than half of our simulations result in differences of 0.004 or less at this wavelength. This translates into errors of approximately 0.04 in retrieved AOT (assuming a ratio of ten to one [34]), which is not so extreme. In the red (0.66 μm), maximum vector-scalar differences are 0.01, but most are less than 0.002. Also plotted in Fig. 5 are the maximum (magnitude) reflectance differences that would still yield AOT within expected MODIS uncertainty over land, defined as $\pm 0.05 \pm 0.2\tau$ [15]. Again, we assumed the ten-to-one AOT-to-reflectance ratio. In more than half our simulations, the neglect of polarization does not lead to extreme errors in retrieved AOT, even in the blue (0.47 μm).

Fig. 4. Errors in retrieved AOT (as a function of input AOT) due to the neglect of polarization in the RT formulation, for each of the sample geometries shown in Fig. 1 (a) at 0.466 μm and (b) at 0.660 μm.

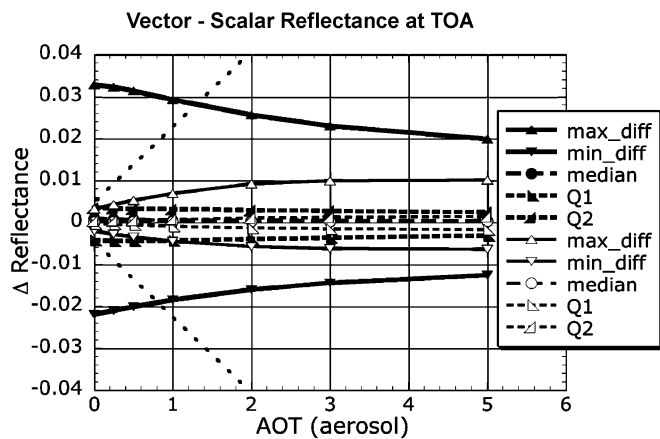


Fig. 5. Maximum, minimum, median, and quartile values of the difference between vector and scalar TOA reflectance, plotted as a function of AOT. Thick curves and closed symbols represent blue ($0.47 \mu\text{m}$), whereas thin curves and open symbols depict red ($0.66 \mu\text{m}$) MODIS channels. The black lines estimate the maximum difference that would lead to AOT retrieved within the expected AOT error ($\Delta\rho \sim ((0.05 + 0.2\tau)/10)$).

Fig. 5 also plots the median reflectance difference for the set of simulated geometry. Median vector-scalar reflectance difference is about -0.0008 in the blue and -0.0002 in the red. These values would introduce approximately $+0.008$ upon the retrieved AOT in the blue, for the simulated geometry in this paper.

In order to determine how the neglect of polarization introduces errors to the climatology of MODIS aerosol retrieval, the simulated geometry must be representative of the MODIS-observed geometry on global and long-term scales. MODIS-atmosphere global data [Level 3 Daily (<http://modis-atmos.gsfc.nasa.gov>)] includes scattering angle histogram data that can be easily aggregated into a year-long histogram (that includes over two billion observations). Fig. 6 plots the year-long probability histogram of the MODIS scattering geometry as compared to the simulated scattering geometry. MODIS from Terra and MODIS from Aqua are plotted separately as well as together. The figure shows that our simulated geometry is sufficiently representative of the observed geometry, and therefore, we conclude that TOA reflectance errors from neglecting polarization would introduce only very small error (~ 0.008) into a global long-term value of MODIS derived AOT over land. It follows that calculations of global radiative forcing, based on the MODIS AOT retrievals, should be nearly independent of presence of polarization within the RT calculations. Global and long-term radiative flux calculations should also be unbiased (e.g., 28).

This means that using a vector code is not necessary for MODIS being useful for deriving aerosol climatology. However, including polarization is very important if MODIS is used to monitor individual aerosol events, such as in application to air quality.

V. DISCUSSION AND CONCLUSION

We have applied a well-known radiative transfer code to study errors of retrieved aerosol optical thickness from MODIS over

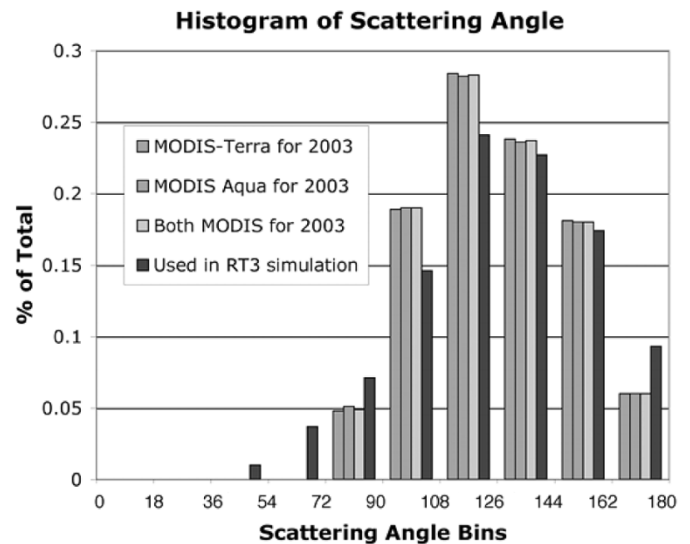


Fig. 6. Histograms of scattering angles simulated by our set of geometry compared to scattering angles observed by MODIS throughout the course of 2003. Terra and Aqua are plotted separately and together.

land, resulting from the neglect of polarization in representing radiative transfer through the atmosphere. In confirmation of Fraser *et al.* [25], the neglect of polarization in the red channel does not usually cause large errors in TOA reflectance. In the red ($0.66 \mu\text{m}$), the Rayleigh optical thickness is small, resulting in little polarization of the signal. Yet in the blue ($0.47 \mu\text{m}$), where Rayleigh optical thickness is much larger, the neglect of polarization can produce large errors for the simulated TOA reflectance. These errors range from near zero when scattering angles are near 135° and up to 0.03 for certain scattering geometry. These errors may be positive or negative depending on the specific scattering geometry. Thus, for specific angles, the neglect of polarization may lead to a AOT retrieval error of 0.3, a very large error, especially in background AOT conditions (< 0.1). This means that users of overland AOT in the $0.47\text{-}\mu\text{m}$ channel, derived from the present MODIS algorithm, should be cautious in applying the data in specific situations. For long-term and global measurements, however, the positive and negative errors generally cancel out. This means that even in its present form, products from the MODIS algorithm can be sufficiently accurate for statistics on large spatial and long temporal scales. Thus, MODIS should be suitable for accurate estimates of aerosol radiative forcing and or fluxes.

ACKNOWLEDGMENT

In addition to the insight received from S. Mattoo and W. Wiscombe, the authors would like to thank R. Fraser for unretiring for a few hours to provide historical context for polarization within the radiative transfer codes. The authors are grateful to P. Colarco for providing the working scripts for running the RT3 and MIEV codes, as well as for help with interpretation of the results. Finally, the authors want to thank the reviewers who gave us deserved criticism and many excellent suggestions.

REFERENCES

- [1] J. T. Houghton, Y. Ding, D. J. Griggs, M. Noguer, P. J. van der Linden, X. Dai, K. Maskell, and C. A. Johnson, Eds., "Intergovernmental Panel on Climate Change (IPCC), Climate change 2001: The scientific basis," in *Contribution of Working Group I to the Third Assessment Report of the Intergovernmental Panel on Climate Change*. Cambridge, U.K.: Cambridge Univ. Press, 2001, pp. 881–881.
- [2] V. Ramanathan, P. J. Crutzen, J. T. Kiehl, and D. Rosenfeld, "Atmosphere—'Aerosols, climate, and the hydrological cycle,'" *Science*, vol. 294, no. 5549, pp. 2119–2124, 2001.
- [3] J. M. Samet, F. Dominici, F. C. Curriero, I. Coursac, and S. L. Zeger, "Fine particulate air pollution and mortality in 20 US cities, 1987–1994," *New Engl. J. Med.*, vol. 343, no. 24, pp. 1742–1749, 2000.
- [4] Y. J. Kaufman, D. Tanre, and O. Boucher, "A satellite view of aerosols in the climate system," *Nature*, vol. 419, no. 6903, pp. 215–223, 2002.
- [5] M. D. King, Y. J. Kaufman, D. Tanre, and T. Nakajima, "Remote sensing of tropospheric aerosols from space: Past, present, and future," *Bull. Amer. Meteorol. Soc.*, vol. 80, no. 11, pp. 2229–2259, 1999.
- [6] V. V. Salomonson, W. L. Barnes, P. W. Maymon, H. E. Montgomery, and H. Ostrow, "MODIS, advanced facility instrument for studies of the earth as a system," *IEEE Trans. Geosci. Remote Sensing*, vol. 27, pp. 145–153, Mar. 1989.
- [7] "EOS AM-1 platform, instruments, and scientific data," *IEEE Trans. Geosci. Remote Sensing*, vol. 36, pp. 1039–1353, July 1998.
- [8] C. L. Parkinson, "Aqua: An earth-observing satellite mission to examine water and other climate variables," *IEEE Trans. Geosci. Remote Sensing*, vol. 41, pp. 173–183, Feb. 2003.
- [9] L. L. Stowe, A. M. Ignatov, and R. R. Singh, "Development, validation, and potential enhancements to the second-generation operational aerosol product at the national environmental satellite, data, and information service of the national oceanic and atmospheric administration," *J. Geophys. Res.*, vol. 102, no. D14, pp. 16923–16934, 1997.
- [10] B. Guenther, X. Xiong, V. V. Salomonson, W. L. Barnes, and J. Young, "On orbit performance of the earth observing system moderate resolution imaging spectroradiometer: First year of data," *Remote Sens. Environ.*, vol. 83, pp. 16–30, 2002.
- [11] Y. J. Kaufman, D. Tanre, L. A. Remer, E. F. Vermote, A. Chu, and B. N. Holben, "Operational remote sensing of tropospheric aerosol over land from EOS Moderate Resolution Imaging Spectroradiometer," *J. Geophys. Res.*, vol. 102, no. D14, pp. 17 051–17 067, 1997.
- [12] D. Tanre, Y. J. Kaufman, M. Herman, and S. Mattoo, "Remote sensing of aerosol properties over oceans using the MODIS/EOS spectral radiances," *J. Geophys. Res.*, vol. 102, no. D14, pp. 16971–16988, 1997.
- [13] R. C. Levy, L. A. Remer, D. Tanre, Y. J. Kaufman, C. Ichoku, B. N. Holben, J. M. Livingston, P. B. Russell, and H. Maring, "Evaluation of the Moderate-Resolution Imaging Spectroradiometer (MODIS) retrievals of dust aerosol over the ocean during PRIDE," *J. Geophys. Res.*, vol. 108, no. D19, 2003.
- [14] L. A. Remer, Y. J. Kaufman, D. Tanre, S. Mattoo, D. A. Chu, J. V. Martins, L. R.-R. C. Ichoku, R. C. Levy, R. G. Kleidman, T. F. Eck, E. Vermote, and B. N. Holben, "The MODIS aerosol algorithm, products and validation," *J. Atmos. Sci.*, 2004, to be published.
- [15] C. Ichoku, D. A. Chu, S. Mattoo, Y. J. Kaufman, L. A. Remer, D. Tanre, I. Slutsker, and B. N. Holben, "A spatio-temporal approach for global validation and analysis of MODIS aerosol products," *Geophys. Res. Lett.*, vol. 29, no. 12, 2002.
- [16] L. A. Remer, D. Tanre, Y. J. Kaufman, C. Ichoku, S. Mattoo, R. Levy, D. A. Chu, B. Holben, O. Dubovik, A. Smirnov, J. V. Martins, R. R. Li, and Z. Ahmad, "Validation of MODIS aerosol retrieval over ocean," *Geophys. Res. Lett.*, vol. 29, no. 12, 2002.
- [17] D. A. Chu, Y. J. Kaufman, C. Ichoku, L. A. Remer, D. Tanre, and B. N. Holben, "Validation of MODIS aerosol optical depth retrieval over land," *Geophys. Res. Lett.*, vol. 29, no. 12, 2002.
- [18] B. N. Holben, T. F. Eck, I. Slutsker, D. Tanre, J. P. Buis, A. Setzer, E. Vermote, J. A. Reagan, Y. J. Kaufman, T. Nakajima, F. Lavenue, I. Jankowiak, and A. Smirnov, "AERONET—A federated instrument network and data archive for aerosol characterization," *Remote Sens. Environ.*, vol. 66, no. 1, pp. 1–16, 1998.
- [19] A. Ignatov, L. Stowe, S. Sakerin, and G. Korotaev, "1995: Validation of the NOAA/NESDIS satellite aerosol product over the north atlantic in 1989," *J. Geophys. Res.*, vol. 100, no. D3, pp. 5123–5132, 1995.
- [20] C. Ichoku, L. A. Remer, Y. J. Kaufman, R. Levy, D. A. Chu, D. Tanre, and B. N. Holben, "MODIS observation of aerosols and estimation of aerosol radiative forcing over southern africa during SAFARI 2000," *J. Geophys. Res.*, vol. 108, no. D13, 2003.
- [21] R. C. Levy, L. A. Remer, J. V. Martins, Y. Kaufman, A. Plana-Fattori, J. Redemann, P. B. Russell, and B. Wenny, "Evaluation of the MODIS aerosol retrievals over ocean and land during CLAMS," *J. Atmos. Sci.*, 2004, to be published.
- [22] M. I. Mishchenko, A. A. Lacis, and L. D. Travis, "Errors induced by the neglect of polarization in radiance calculations for Rayleigh-scattering atmospheres," *J. Quant. Spectrosc. Radiat. Transf.*, vol. 51, pp. 491–510, 1994.
- [23] K. N. Liou, *An Introduction to Atmospheric Radiation*, 2nd ed. San Diego: Academic Press, 2002, pp. 577–577.
- [24] H. C. Van de Hulst, *Light Scattering by Small Particles*. New York: Dover, 1984.
- [25] S. Chandrasekhar, *Radiative Transfer*. London, U.K.: Clarendon, 1950.
- [26] J. V. Dave, "Intensity and polarization of radiation emerging from a plane-parallel atmosphere containing monodispersed aerosols," *Appl. Opt.*, vol. 9, no. 12, pp. 2673–2687, 1970.
- [27] R. S. Fraser, R. A. Ferrare, Y. J. Kaufman, and S. Mattoo, "Algorithm for atmospheric corrections of aircraft and satellite imagery," NASA GSFC, Greenbelt, MD, NASA Tech. Memo. 100 751, 1989.
- [28] A. A. Lacis, J. Chowdhary, M. I. Mishchenko, and B. Cairns, "Modeling errors in diffuse-sky radiation: Vector vs. scalar treatment," *Geophys. Res. Lett.*, vol. 25, no. 2, pp. 135–138, 1998.
- [29] K. F. Evans and G. L. Stephens, "A new polarized atmospheric radiative-transfer model," *J. Quant. Spect. Radiat. Transf.*, vol. 46, no. 5, pp. 413–423, 1991.
- [30] W. Wiscombe, "Improved Mie scattering algorithms," *Appl. Opt.*, vol. 19, pp. 505–1519, 1980.
- [31] P. R. Colarco, O. B. Toon, O. Torres, and P. J. Rasch, "Determining the UV imaginary index of refraction of saharan dust particles from total ozone mapping spectrometer data using a three-dimensional model of dust transport," *J. Geophys. Res.*, vol. 107, no. D16, 2002.
- [32] J. Lenoble and C. Brogniez, "A comparative review of radiation aerosol model," *Beitr. Phys. Atmos.*, vol. 57, no. 1, pp. 1–20, 1984.
- [33] R. A. McClatchey *et al.*, "Optical properties of the atmosphere," in *Environmental Research Papers*, L. G. H. Fiel *et al.*, Ed. Bedford, MA: Air Force Cambridge Res. Lab., Hanscom Air Force Base, 1971. AFCRL-TR-71-0279.
- [34] Y. J. Kaufman, A. E. Wald, L. A. Remer, B.-C. Gao, R.-R. Li, and L. Flynn, "The MODIS 2.1- μm channel—Correlation with visible reflectance for use in remote sensing of aerosol," *IEEE Trans. Geosci. Remote Sensing*, vol. 35, pp. 1286–1298, Sept. 1997.



Robert C. Levy received the B.A. degree in mathematics from Oberlin College, Oberlin, OH, in 1994, and the M.S. degree in atmospheric science from Colorado State University, Fort Collins, in 1996. He is currently pursuing the Ph.D. degree in meteorology at the University of Maryland, College Park.

Since 1998, he has been with Science Systems and Applications, Inc., Lanham, MD, working on-site within the Climate and Radiation Branch, Goddard Space Flight Center, Greenbelt, MD. He supports the EOS–MODIS science team and focuses

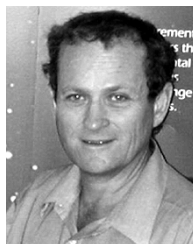
on validation and development of the MODIS aerosol retrieval algorithms. Some of his current research involves customizing the retrieval over the U.S. east coast, in order for MODIS to help monitor air pollution in the region. He has been involved in major field campaigns including the Puerto Rico Dust Experiment (PRIDE) and the Chesapeake Lighthouse Airborne Measurements for Satellites (CLAMS).



Lorraine A. Remer received the B.S. degree in atmospheric science from the University of California, Davis, the M.S. degree in oceanography from the Scripps Institution of Oceanography, San Diego, CA, and the Ph.D. degree in atmospheric science from the University of California, Davis.

She has been with the National Aeronautics and Space Administration, Goddard Space Flight Center (GSFC), Greenbelt, MD, since 1991, employed by Science Systems and Applications, Inc., Lanham, MD, until 1998, when she became a civil servant.

She is currently a Physical Scientist with the Climate and Radiation Branch, Laboratory for Atmospheres, GSFC. She is a Member of the EOS-MODIS science team and was a member of the Global Aerosol Climatology Project science team. Her current research interests are the climatic effects and remote sensing of atmospheric aerosol. She has been involved in several field campaigns including the Smoke/Sulfate, Cloud And Radiation (SCAR) experiments, the Tropospheric Aerosol Radiative Forcing Observational Experiment (TARFOX), the Israeli Desert Transition Zone experiment, the Puerto Rico Dust Experiment (PRIDE), and the Chesapeake Lighthouse Airborne Measurements for Satellites (CLAMS).



Yoram J. Kaufman received the B.S. and M.S. degrees in physics from the Technion—Israeli Institute of Technology, Haifa, Israel, and the Ph.D. degree from Tel-Aviv University, Tel-Aviv, Israel.

He came to NASA Goddard Space Flight Center (GSFC), Greenbelt, MD, in 1979 on an NRC Fellowship Award. He is currently a Senior Fellow and Atmospheric Scientist at GSFC. He has served as the Project Scientist of the Earth Observing System first satellite EOS-Terra, from 1996 through its launch in December 1999, and was a Member of the MODIS

Science Team (1988–2003). He works on remote sensing of aerosol, studying aerosol interaction with clouds and radiation and impact on climate. He conducted the Smoke/Sulfate, Clouds And Radiation (SCAR) field experiments in Brazil and the U.S. (1993–1995), to characterize smoke aerosol properties, their emissions from fires, and their effect on clouds and radiation. He has over 170 refereed publications.

Dr. Kaufman is the seventh recipient of the NASA/GSFC Nordberg Award for Earth Sciences and was awarded the NASA Medal for Exceptional Scientific Achievement.